

Hierarchical intra-network organization of the visual network from resting-state fMRI data

Yanlu Wang¹ and Tie-Qiang Li^{1,2}

¹Clinical Sciences, Intervention and Technology, Karolinska Institute, Stockholm, Stockholms Län, Sweden, ²Medical Physics, Karolinska University Hospital, Huddinge, Stockholms Län, Sweden

Introduction

We have previously developed a voxel-based analysis framework to extract functional connectivity networks from whole-brain resting-state functional magnetic resonance imaging (fMRI) data using hierarchical clustering approach. Hierarchical clustering naturally stratifies the correlation coefficient matrix derived from dynamic fMRI data into a hierarchical structure that may reflect the functional organization of the functional connectivity networks.

Purpose

To utilize the inherent property of hierarchical clustering algorithm to stratify data into a hierarchical structure and investigate the sub-network organization of resting-state functional connectivity networks.

Methods

The visual network extracted from a previous study¹ was further sub-divided using hierarchical clustering. The visual network was further sub-divided by systematically increasing the cut level of the hierarchy tree (dendrogram). This was done up to cut level $k=80$, where the node's inconsistency coefficient (IC) fell within one standard deviation from the mean IC value. All cuts that resulted in children clusters of relatively equal size in relative to the mother cluster and are themselves significantly large in size (<20 voxels from cluster simulations) were automatically labeled as "dissociable nodes" for visual inspection to determine whether they are functional sub-divisions of the network. The "dissociable nodes" that were determined to be functional sub-divisions through visual inspection were used to reconstruct the network's functional hierarchical tree.

Results

The mean of the inconsistency coefficients at full depth is 1.95 ± 0.47 . This corresponds to termination at cut level 80 for the network. Systematic sub-division of the dendrogram resulted in 14 divisible nodes corresponding to 15 sub-networks. The functional sub-divisions organized hierarchically are shown in figure 1. The Sub-networks and their relative associations in the visual network correspond well to the two-stream hypothesis of visual processing².

Discussion

Central to the visual network, and the sub-network with the lowest height is the primary visual cortex and higher order visual areas (fig.1, cluster 1,2). The functional sub-division of the visual network reflects the two-stream hypothesis for visual processing, with distinct functional sub-divisions corresponding to the ventral stream and the dorsal stream areas. Consistent to the two-stream hypothesis, regions corresponding to the dorsal stream are more closely associated to the primary visual cortex than regions corresponding to the ventral stream (fig.1).

The dorsal stream is responsible for detecting motion, locating objects in space, and processing visual information used to guide movements. The sub-network with the least distance (Table I, height=0.747) in the dorsal stream is anterior to the primary visual cortex (fig.1, cluster 3) is responsible for visual association and detection of motion. Sub-networks occupying more anterior regions of the dorsal stream (fig.1, cluster 4,5) have higher distances (Table I, height=0.754. These regions are responsible for cognitive/associative tasks such as memory retrieval, and self-awareness³.

The sub-network with the shortest distance in the ventral stream is the fusiform gyrus (fig. 1, clusters 6-9). It is responsible for processing high-order visual information such as colors, words, and numbers⁴. The fusiform gyrus is followed by the inferior temporal cortex (fig.1, clusters 10-12), which is responsible for visual object recognition and is considered to be the final stage in the ventral cortical visual system. The region with largest distance in the visual network corresponds to the middle temporal gyrus (fig.1, clusters 13-15), which has been connected to different higher-order processes such as accessing word meaning while reading.

Further subdivisions to higher cut levels might reveal additional functional associations. Also, other resting-state functional connectivity networks may also be functionally sub-divided in the same fashion to reveal their intrinsic hierarchical organization. This will be investigated further in the future studies.

Conclusion

The extracted functional hierarchy of the visual networks is reminiscent of the two-stream hypothesis. This indicates that hierarchical clustering algorithm can be used to extract intra-network connectivity from resting-state fMRI data that reflects functional sub-division of resting-state functional connectivity networks.

References

1. Wang, Y.L. and T.Q. Li, Analysis of Whole-Brain Resting-State fMRI Data Using Hierarchical Clustering Approach. Plos One, 2013. **8**(10).
2. Ungerleider, L.G., *Two cortical visual systems*. Analysis of visual behavior, 1982: p. 549-586.
3. Astafiev, S.V., et al., *Extrastriate body area in human occipital cortex responds to the performance of motor actions*. Nature neuroscience, 2004. **7**(5): p. 542-548.
4. Creem, S.H. and D.R. Proffitt, *Defining the cortical visual systems: "what", "where", and "how"*. Acta Psychol, 2001. **107**(1-3): p. 43-68.

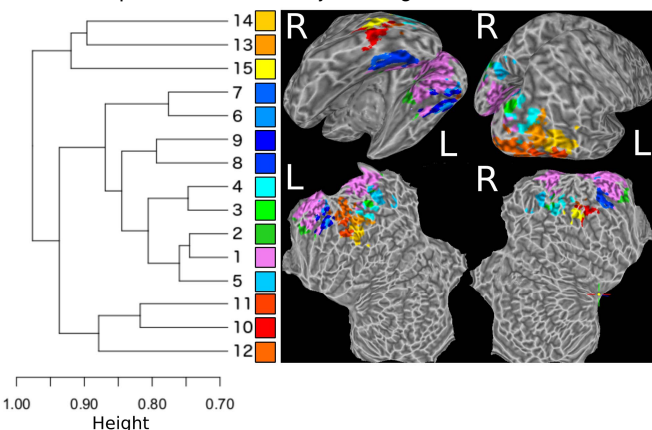


Figure 2: Hierarchical intra-network connectivity of the visual network. Left: The functional hierarchical tree for the visual network. The clusters are numbered by order of increasing height. Right: Clusters overlaid on inflated and flat 3D renders. The clusters' colors correspond to the color-coding in the hierarchical tree.

Table II: Sub-network cluster information. Cluster sizes in voxel count, heights to their mother nodes, and focus point (center of mass) in Talairach-Tournoux space. The clusters' labeling corresponds the labeling found in figure 1.

Cluster Number	Size	Height	Focus Point (LPI) TLRC
1	546	0,745	(3, -74, 1)
2	62	0,745	(16, -49, -4); (-15, -53, -4)
3	37	0,747	(18 -81, 25); (-18 -82, 24)
4	87	0,747	(-27, -83, 16); (30, -77, 22)
5	86	0,76	(14, -74, 29); (-11, -78, 29)
6	150	0,776	(4, -74, -20)
7	36	0,776	(-32, -66, -22)
8	48	0,794	(-23, -75, -14)
9	47	0,794	(26, -74, -12)
10	33	0,818	(-41, -72, -1)
11	41	0,818	(45, -67, -2)
12	64	0,879	(32, -83, -1); (-34, -82, 0)
13	45	0,896	(40, -73, 19)
14	59	0,896	(48, -61, 7)
15	33	0,92	(-40, -73, 12)